Check for updates

RESEARCH ARTICLE

Numerical model of aluminothermic reduction vessel preheating and charge heating with graphite heating rods

[version 1; peer review: 2 approved]

Sergey Semenov[1], Patrick Namy[1], Aditya Kale[2], Sello Tsebe[2]

[1]SIMTEC, Grenoble, 38000, France
[2]MINTEK, Randburg, 2194, South Africa

v1 **First published:** 22 Nov 2024, **4**:253
https://doi.org/10.12688/openreseurope.18586.1
Latest published: 22 Nov 2024, **4**:253
https://doi.org/10.12688/openreseurope.18586.1

Abstract

Background

The present work is conducted in the framework of the SisAl Pilot EU project, which aims to optimize silicon production in Europe by recycling materials and using carbon-emission-friendly technology. Silicon production experiments were conducted on laboratory and pilot scales in different types of furnaces, including reduction vessels used as chemical reactors for molten slag-metal mixtures. In addition to experimental work, process optimization also relies on numerical modelling.

Methods

In this study, COMSOL Multiphysics® was used for numerical testing of new thermal and electrical designs of a reduction vessel by simulating its preheating and charge heating with three graphite heating rods powered by a three-phase alternating current transformer. A one-heating-rod design is also tested.

Results and conclusions

The model predicts that available electrical equipment is sufficient for preheating the empty reduction vessel up to 1600°C in less than 4 h. Owing to the model, the geometry of the heating rod was optimized to maintain its temperature below 2500°C. However, it was found that a modification of the electrical equipment would be required to heat the vessel charge with the heating rods submerged into it.

Open Peer Review

Approval Status ✓ ✓

	1	2
version 1 22 Nov 2024	✓ view	✓ view

1. **Kagan Benzesik**, Istanbul Technical University, Istanbul, Turkey

2. **Mickaël Antoni**, Aix-Marseille Université, Marseille, France

Any reports and responses or comments on the article can be found at the end of the article.

Keywords
Reduction Vessel Preheating, Charge Heating, Graphite Heating Rods, Aluminothermic Reduction, Finite Element Method, COMSOL Multiphysics, Heat Transfer Modelling, Phase Change



This article is included in the Horizon 2020 gateway.

Corresponding author: Sergey Semenov (sergey.semenov@simtecsolution.fr)

Author roles: Semenov S: Writing – Original Draft Preparation; **Namy P**: Writing – Review & Editing; **Kale A**: Conceptualization; **Tsebe S**: Conceptualization

Competing interests: No competing interests were disclosed.

Grant information: This project has received funding from the European Union's Horizon 2020 research and innovation programme under grant agreement No 869268 (project name SisAl Pilot).

Copyright: © 2024 Semenov S *et al*. This is an open access article distributed under the terms of the Creative Commons Attribution License, which permits unrestricted use, distribution, and reproduction in any medium, provided the original work is properly cited.

How to cite this article: Semenov S, Namy P, Kale A and Tsebe S. **Numerical model of aluminothermic reduction vessel preheating and charge heating with graphite heating rods [version 1; peer review: 2 approved]** Open Research Europe 2024, **4**:253 https://doi.org/10.12688/openreseurope.18586.1

First published: 22 Nov 2024, **4**:253 https://doi.org/10.12688/openreseurope.18586.1

1. Introduction

This work was conducted in the framework of the SisAl Pilot EU project, which is focused on demonstrating the possibility of metallurgical-grade silicon production at the pilot scale based on the aluminothermic reduction of silica. In comparison with the traditional carbothermic reduction of silica, the advantage of the proposed technology is its low CO2 emissions. As part of the project, the numerical modelling support of the experimental works was stipulated. One of the efforts focused on developing a numerical model of a new reduction vessel design proposed by MINTEK as a metallurgical reactor for the aluminothermic reaction between metal and slag. The objective of the present modelling work is to test the thermal and electrical performance of the new vessel design during preheating and aluminothermic reduction. The following hypotheses need to be tested: 1) the possibility of preheating the reduction vessel up to 1600°C in less than 4 h by using an existing MINTEK electrical equipment, while maintaining the temperature of graphite heating rods below 2500°C; 2) the possibility of continuous charge heating with help of three graphite heating rods submerged in the melt; 3) the risk of slag solidification during the aluminothermic reduction in the absence of external heating. In Section 2 and Section 3, the model geometry and numerical methods are described, respectively. Section 4 and Section 5 present the governing equations and material properties, respectively. In Section 6, numerical results are presented and discussed. Finally, Section 7 concludes the paper.

2. Problem geometry

As shown in Figure 1, the reduction vessel has a cylindrical shape with 120° sector symmetry. It consists of a graphite crucible containing the vessel charge and gas, three graphite heating rods placed symmetrically around the axis of rotation, refractory layers, and the steel shell separated from the refractory by a calcium silicate board and a ceramic fiber blanket. The thermal part of the problem benefits from 120° sector symmetry, and therefore is resolved within only one 120° sector (see Figure 1). However, the electrical part of the problem has no sector symmetry because of the electrical contact between the three electrical phases via the electrically conducting vessel charge. Consequently, a complete 3D geometry was modelled for the electrically conducting parts of the vessel, including the vessel charge, crucible, and three heating rods. The heating rod geometry (see Figure 2) is based on existing equipment at Elkem, one of the project partners, and is given three adjustable parameters *a*, *b* and *c* to have some degrees of freedom for the problem optimization.

3. Methods

The problem was numerically solved using the finite element software COMSOL Multiphysics® version 6.0 (www.comsol.com, a copyright license is obtained). The following modules have been used to set up the model physics: Heat Transfer in Solids and Fluids with phase change and convectively enhanced conductivity while fluid flow is not directly simulated, Surface-to-Surface Radiation, and Electric Currents to simulate the Joule effect in electrically conducting materials. Bidirectional coupling of all modules is present owing to multiple interdependencies via material properties. Each field was spatially discretized using linear Lagrange elements. Time integration is performed with a Backward Differentiation Formula (BDF) of orders 1 to 2. The computational domain is spatially discretized with a quadrilateral mesh that consists of 1 195 000 finite elements, as shown in Figure 3, resulting in 2 570 000 degrees of freedom. The computations were performed on two laptops with eight physical cores, an Intel processor with 64 GB RAM, and a workstation with 64 physical cores and 1 TB RAM.

4. Governing equations

4.1. Electric current equation

One of the requirements imposed by the reduction vessel design is the use of a 3-phase alternating current (AC) power source, such as an electrical transformer available at MINTEK. Thus, the present model implements AC electrical equations

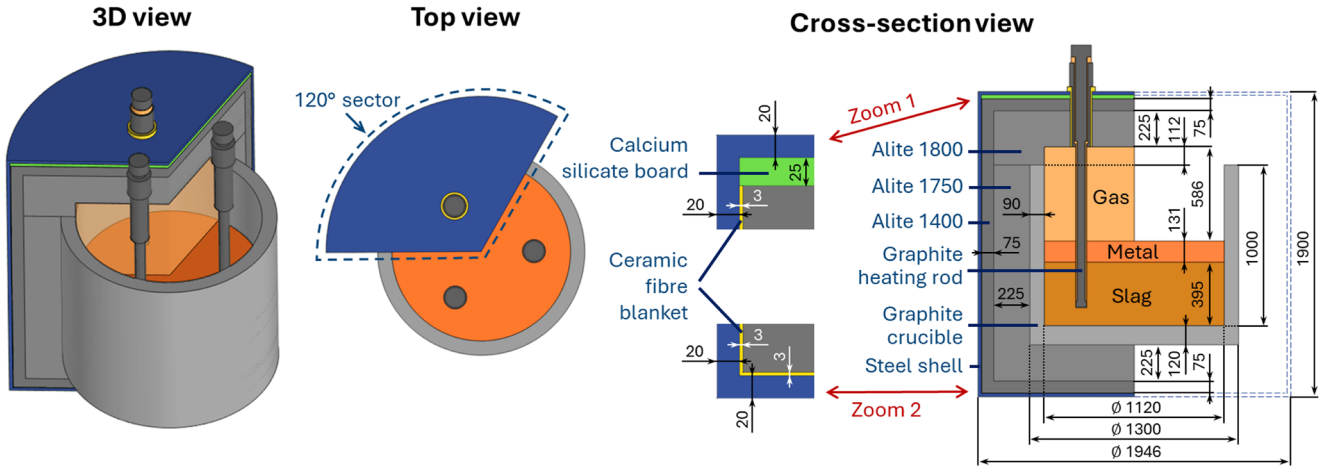

Figure 1. Modelled reduction vessel geometry and materials. Dimensions in mm.

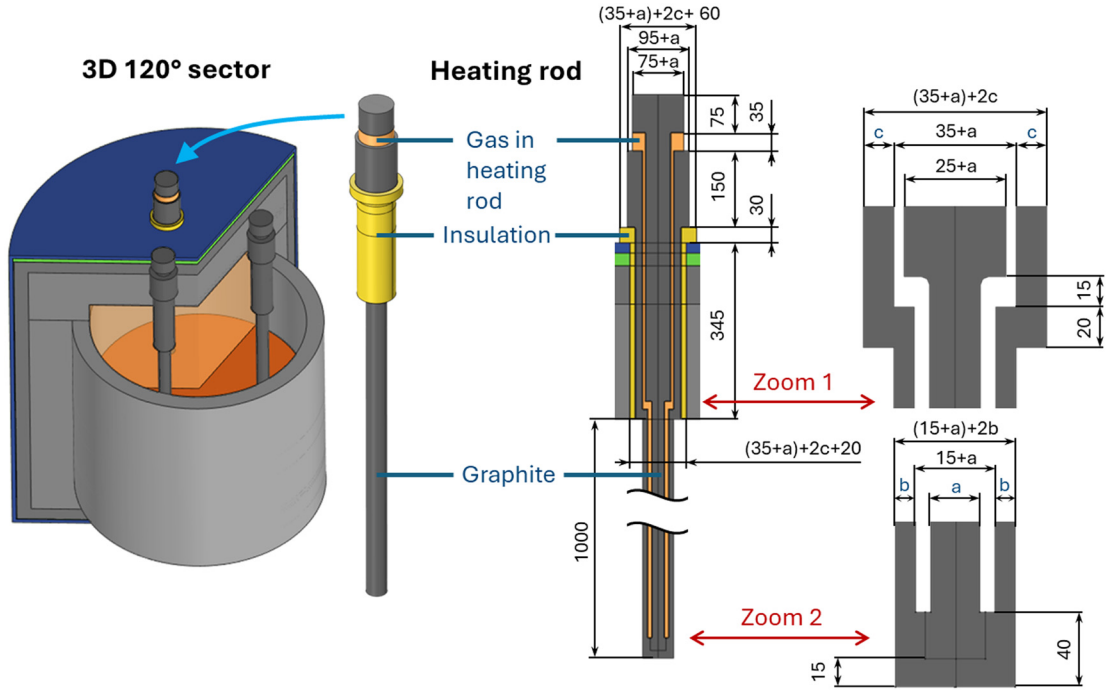

Figure 2. Heating rod geometry and materials. Dimensions in mm.

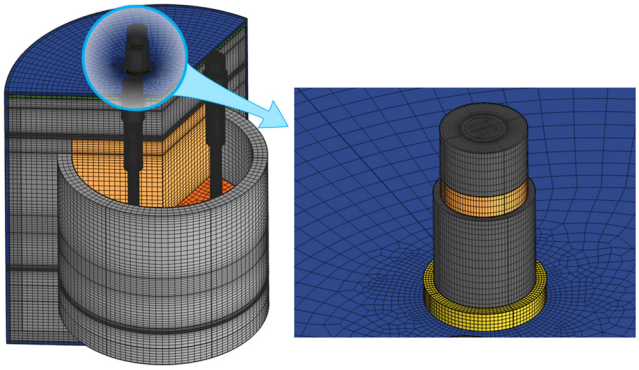

Figure 3. Spatial discretization mesh.

in the frequency domain formulation. The equations of current conservation are solved for all electrically conducting domains (metal, slag, crucible, and three heating rods):

$$\nabla \cdot \mathbf{j} = 0, \qquad \mathbf{j} = \sigma \mathbf{E} + j\omega \mathbf{D},$$

$$\mathbf{E} = -\nabla V, \qquad \mathbf{D} = \varepsilon_0 \varepsilon_r \mathbf{E}, \qquad \omega = 2\pi f$$

where $\mathbf{j}$ is the complex amplitude (or phasor) of the electric current density, $\mathbf{E}$ is the phasor of the electric field, V is the phasor of the electric potential, $\mathbf{D}$ is the phasor of the electric displacement field, σ is the electrical conductivity as a function of temperature, f is the alternating current frequency, ω is the angular frequency, ε_0 is the vacuum permittivity, ε_r is the relative permittivity, and $j = \sqrt{-1}$ is the imaginary unit. The volume density of the heat source owing to the Joule effect is expressed as follows:

$$Q = \frac{1}{2}\mathrm{Re}(\mathbf{j} \cdot \mathbf{E}^*)$$

where asterisk $\mathbf{E}^*$ denotes the complex conjugate of $\mathbf{E}$, and Re(Z) is the real part of the complex number Z. The electrical boundary conditions on the heating rod terminals (see Figure 4) are defined by an electrical transformer that powers the vessel and by the type of 3-phase electrical connection of the heating rods: either delta (D) or star (Y) connection. Here, U_L and I_L are the effective line voltage and effective line current, U_{hr}^{Δ} and I_{hr}^{Δ} are the effective voltage and effective current through a heating rod in the delta configuration

$$U_{hr}^{\Delta} = U_L, \qquad I_{hr}^{\Delta} = I_L/\sqrt{3}$$

and U_{hr}^{*} and I_{hr}^{*} are those in the star configuration:

$$U_{hr}^{*} = U_L/\sqrt{3}, \qquad I_{hr}^{*} = I_L$$

The boundary conditions for the electric potential at the top terminals are as follows:

$$V_{i_{top}} = \sqrt{2}U_{hr}^{*}e^{j\varphi_i} = \frac{\sqrt{2}}{\sqrt{3}}U_L e^{j\varphi_i}, \qquad i = 1,2,3$$

with line phases $\varphi_i = i \cdot 120°$. For the bottom terminals, in case of star connection:

$$V_{i_{bot}} = V_{i_{bot}}^{*} = 0, \qquad i = 1,2,3$$

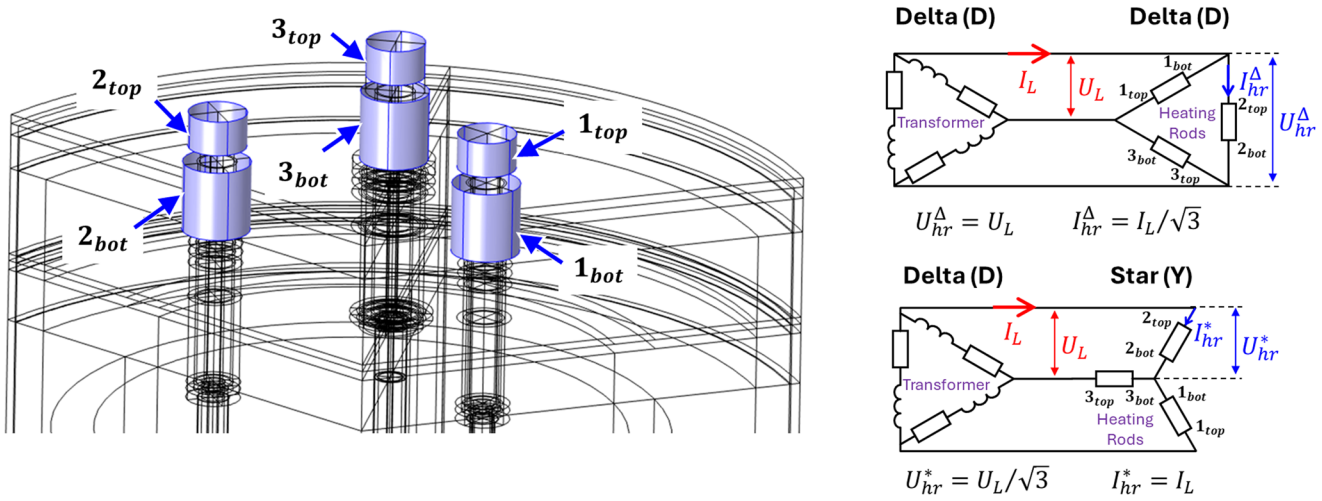

Figure 4. Heating rod terminals and connection types.

and in case of delta connection:

$$V_{i_{bot}} = V_{i_{bot}}^{\Delta} = \frac{\sqrt{2}}{\sqrt{3}} U_L e^{j(\varphi_i + 120°)}, \qquad i = 1,2,3$$

Electric insulation is assumed on other external boundaries of the electrically conducting domain:

$$\mathbf{j} \cdot \mathbf{n} = 0$$

4.2. Heat transfer with surface-to-surface radiation

The following heat equation is solved for all domains of the 120° sector, as shown in Figure 1.

$$\rho c_p' \frac{\partial T}{\partial t} + \nabla \cdot \mathbf{q} = Q, \qquad \mathbf{q} = -\max(1, \mathrm{Nu}) \cdot k \nabla T$$

where T is the temperature, t is the time, ρ is the density, $\mathbf{q}$ is the convectively enhanced conductive heat flux, k is the thermal conductivity, c_p' is the isobaric specific heat capacity modified with the Apparent Heat Capacity method to account for phase changes, Q is the volume density of the heat source due to the Joule effect in electrically conducting materials and the heat loss in the crucible gas due to a protective gas flow with a modelled rate of 8 L/min. The conductivity k is convectively enhanced in the crucible gas with the Nusselt number Nu, which is computed according to an empirical model as a function of the temperature difference between the heating rod and crucible. A zero normal heat flux was imposed on the two symmetry planes, as shown in Figure 5 (a).

$$\mathbf{q} \cdot \mathbf{n} = 0$$

where $\mathbf{n}$ is the unit vector normal to the plane. As the electrical cables connected to the heating rods are supposed to be water-cooled, the ambient temperature T_{amb} is imposed on the heating rod terminals, as shown in Figure 5 (b).

$$T = T_{amp}$$

On the other external surfaces of the vessel, as shown in Figure 5 (c), the heat flux owing to external natural convection is applied:

$$\mathbf{q} \cdot \mathbf{n} = h(T - T_{amp})$$

where $\mathbf{n}$ is the outward unit normal vector and h is the heat transfer coefficient computed according to several empirical models of external natural convection: one for a thin vertical cylinder and two models for the upper and lower horizontal plates. The temperature continuity on all material interfaces was applied as follows:

$$T_{up} = T_{down}$$

where the subscripts *up* and *down* denote opposite sides of the interface, with *up* corresponding to the positive direction of the normal vector $\mathbf{n}$. The condition of the heat flux continuity/discontinuity at the material interfaces is written as follows:

$$\mathbf{q}_{up} \cdot \mathbf{n} - \mathbf{q}_{down} \cdot \mathbf{n} = q$$

where q denotes the surface density of the interfacial heat source in W/m^2. In the presence of both the metal and slag, an interfacial heat source q at the metal-slag interface due to aluminothermic reduction is computed based on the reaction energy and reaction time. The interfaces adjacent to the gases (in the crucible and in the heating rod) participate in the surface-to-surface radiation and thus have the following interfacial heat source q:

$$q = \varepsilon(G_{rad} - \sigma_{SB} T^4)$$

where ε is the hemispherical emissivity of the radiating surfaces, σ_{SB} is the Stefan-Boltzmann constant, and G is the surface irradiance (surface density of the radiant flux in W/m^2, which arrives at the surface). A special 120° rotation symmetry condition was applied for the surface-to-surface radiation problem, which is not equivalent to a conventional zero-flux symmetry condition but allows radiant heat fluxes to pass through the symmetry planes.

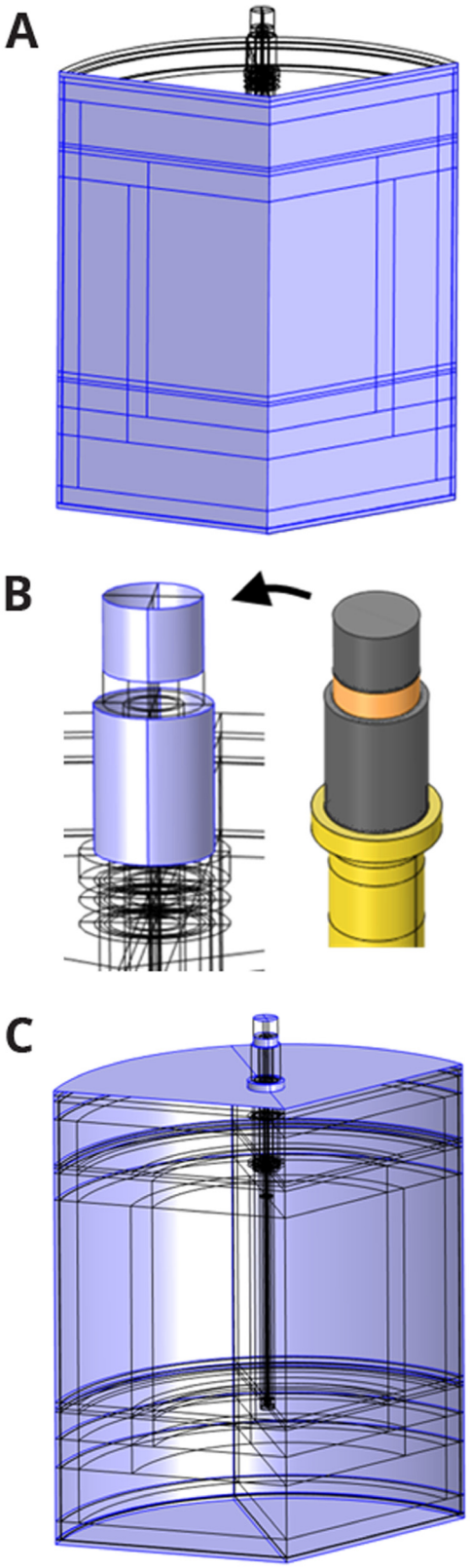

Figure 5. In blue: (a) two symmetry planes, (b) heating rod terminals, (c) other external boundaries of the vessel.

5. Material properties and parameters

5.1. Graphite

For simplicity, the graphite model uses its porosity ϕ, including both open and closed pores, as a single adjustable parameter of the material, which, along with temperature T, defines all other properties of the material. We also assume that the porosity ϕ does not change with temperature T. The graphite density ρ_{gr} is modelled as a linear function of the porosity ϕ:

$$\rho_{gr}(T,\phi) = (1-\phi)\rho_C(T)$$

where $\rho_C(T)$ is the density of non-porous graphite, which is modelled as a function of temperature using the linearized thermal expansion coefficient:

$$\alpha_V(T) = -\frac{1}{\rho_C(T)}\left(\frac{\partial \rho_C(T)}{\partial T}\right)_p = \alpha_{V,\mathrm{ref}} + (\alpha_V)'_T(T - T_{\mathrm{ref},\alpha})$$

and the theoretical density of non-porous graphite at a given temperature:

$$\rho_{C,\mathrm{ref}} = 2260\,\mathrm{kg/m^3} \quad \text{at} \quad T_{\mathrm{ref},\rho} = 293\,\mathrm{K}$$

Assuming constant pressure $p = const$ and integrating both sides of $\alpha_V(T)$ expression, we get:

$$\rho_C(T) = \rho_{C,\mathrm{ref}} \exp\left(-\alpha_V(T)\theta + (\alpha_V)'_T \frac{\theta^2}{2}\right)$$

where $\theta = T - T_{\mathrm{ref},\rho}$. Using the above theoretical density model $\rho_{gr}(T,\varphi)$ and fitting the value, slope, and second derivative of the temperature-dependent graphite density found in the literature[1] (see Figure 6), we obtain the theoretical porosity φ of the given material samples (see Figure 6), as well as the following thermal expansion constants:

$$\alpha_{V,\mathrm{ref}} = 1.4508\times10^{-5}\,\mathrm{K^{-1}} \quad \text{at} \quad T_{\mathrm{ref},\alpha} = 293\,\mathrm{K}$$

$$(\alpha_V)'_T = 6.9518\times10^{-9}\,\mathrm{K^{-2}}$$

The specific heat capacity of graphite at a constant pressure $c_{p,gr}(T)$ is assumed to be independent of the material porosity:

$$c_{p,gr}(T) = \begin{cases} c_{p,\mathrm{cub}}(T), & T \le T_1 = 300\,\mathrm{K} \\ c_{p,\mathrm{app}}(T), & T > T_1 = 300\,\mathrm{K} \end{cases}$$

where $c_{p,\mathrm{app}}(T)$ approximates literature data:

$$\begin{aligned} c_{p,\mathrm{app}}(T) = {} & -5.8068\times10^{-17}\cdot \mathrm{T}^6 + 6.8603\times10^{-13}\cdot T^5 \\ & - 3.2774\times10^{-9}\cdot T^4 + 8.1193\times10^{-6}\cdot T^3 \\ & - 1.1138\times10^{-2}\cdot T^2 + 8.4443\cdot T - 1.0091\times10^3 \end{aligned}$$

and $c_{p,\mathrm{cub}}$ is the cubic continuation of $c_{p,\mathrm{app}}$:

$$c_{p,\mathrm{cub}}(T) = \left.\frac{dc_{p,\mathrm{app}}(T)}{dT}\right|_{T=T_1}(T-T_1)\frac{T^2}{T_1^2} + c_{p,\mathrm{app}}(T_1)\left(3 - \frac{2T}{T_1}\right)\frac{T^2}{T_1^2}$$

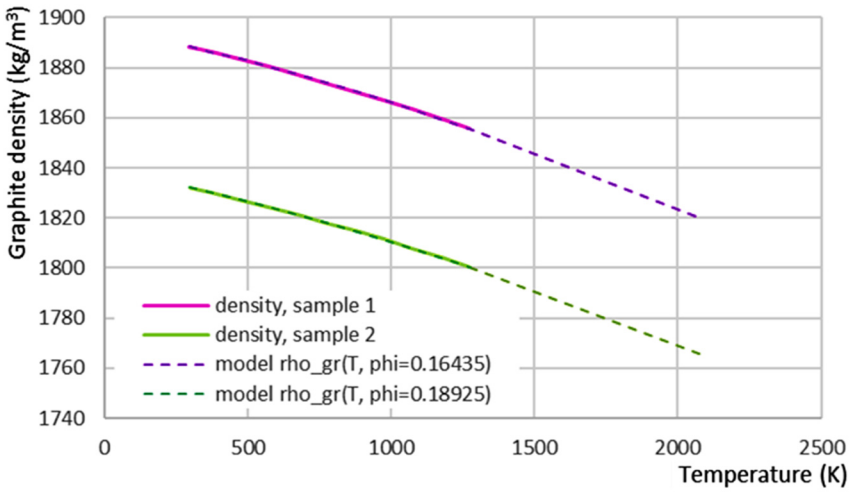

Figure 6. Fitting graphite density from literature[1] (samples 1 and 2) with the theoretical density model.

where T is in K and $c_{p,\mathrm{app}}$ and $c_{p,\mathrm{cub}}$ are in J/kg/K. The thermal k_{gr} and electrical conductivity σ_{gr} of graphite are modelled as functions of its porosity ϕ using Landauer's model of conductivity of a porous medium based on the effective medium percolation theory[2]:

$$k_{gr}(T,\phi) = f_L(k_C(T), k_{air}(T), \phi)$$

$$\sigma_{gr}(T,\phi) = f_L(\sigma_C(T), 0, \phi)$$

where $k_C(T)$ and $\sigma_C(T)$ are the thermal and electrical conductivities of nonporous graphite, respectively, $k_{air}(T)$ is the thermal conductivity of air trapped inside the pores, and f_L is given by 2

$$f_L(k_s,k_p,\phi) = \frac{1}{4}\left(s + \sqrt{s^2 - 8k_sk_p}\right)$$

$$s = k_p(3\phi - 1) + k_s(2 - 3\phi)$$

where k_s and k_p are the solid and pore conductivity, respectively. The temperature dependencies of the non-porous graphite conductivities $k_C(T)$ and $\sigma_C(T)$ were obtained by fitting the graphite conductivities found in the literature[1,3] with the theoretical models $k_{gr}(T, \phi)$ and $\sigma_{gr}(T, \phi)$, where the porosity ϕ is already known from density fitting. Several curves of $k_C(T)$ and $\sigma_C(T)$ obtained in this manner were then averaged, resulting in the following dependencies:

$$k_C(T) = 46758\,\mathrm{W/(m\cdot K)} \cdot (T/1\mathrm{K} + 405)^{-0.8543}$$

$$\begin{aligned}\sigma_C(T) = {} & -7.1142\times10^{-15}\cdot T^6 + 6.5797\times10^{-11}\cdot T^5 \\ & - 2.50415\times10^{-7}\cdot T^4 + 5.2414\times10^{-4}\cdot T^3 \\ & - 0.67881\cdot T^2 + 509.18\cdot T + 6743.35\end{aligned}$$

where T is in K and σ_C is in S/m. In the working range of vessel temperatures, the hemispherical emissivity of graphite ε_C varies between 0.5 and 0.85[3]. The value of ε_C = 0.5 is used in the current model as it corresponds to the worst-case scenario when the heating rod overheats faster. If we can avoid overheating for ε_C = 0.5, we will also avoid it for larger values of ε_C. The relative permittivity of graphite $\varepsilon_{r,gr}$ is taken as the volume average of non-porous graphite $\varepsilon_{r,C}$ = 15 and that of air $\varepsilon_{r,air}$ = 1:

$$\varepsilon_{r,gr} = (1-\phi)\varepsilon_{r,C} + \phi\varepsilon_{r,air}$$

Thus, two types of graphite, one for the crucible and the other for the heating rod, were assumed to be different only by their porosity. The porosity was calibrated by fitting the experimental data for another vessel at Elkem, which used the same graphite materials:

$$\phi_{\mathrm{crucibe}} = 0, \qquad \phi_{\mathrm{heating\,rod}} = 0.08$$

5.2. Slag and metal

The metal phase, which is initially pure Al, becomes an Al-Si-Ca alloy as it reacts with the slag. Similarly, initially SiO_2-CaO slag becomes Al_2O_3-SiO_2-CaO slag as it reacts with the metal. Thus, the slag and metal densities are computed as functions of the temperature T and composition X_i (mole fraction of component i):

$$\rho(T, X_i) = \sum_i [X_i M_i] / \left(\sum_i [X_i V_{m,i}(T)] + V^{EX}\right)$$

where M_i and $V_{m,i}$ are the molar mass and molar volume[4–7] of component i, V^{EX} is a corrective interaction term[7]; i = Al, Si, Ca for the metal; and i = Al_2O_3, SiO_2, CaO for the slag. The composition of the slag and metal is modelled as a function of the relative reaction extent ξ_{rel} which equals 0 at the beginning of the process and 1 at the end of the reaction:

$$X_i = X_{i,init} + \xi_{rel}(X_{i,final} - X_{i,init})$$

For simplicity, it was assumed that the relative reaction extent ξ_{rel} is a linear function of time.

$$\xi_{rel} = t / t_r$$

where t_r is the user-defined reaction time. The initial $X_{i,init}$ and final $X_{i,final}$ compositions, as well as the reaction energy, were estimated using the software provided by the project partner SINTEF. This artificial neural network-based tool[8,9] was trained on FactSage® data for the metal-slag system of interest. Other metal properties, such as thermal and electrical conductivity[4], dynamic viscosity[10], and heat capacity at constant pressure, were computed as for pure aluminum. The thermal conductivity of the slag was assumed to be constant and equal to 1 W/m/K. Other properties of the slag phase, such as heat capacity, enthalpy, viscosity, and electrical conductivity, were computed as functions of temperature T and composition X_i according to the Ken Mills model[11].

5.3. Other materials

The heating rod gas was air and the crucible gas was argon. The densities were computed according to the ideal gas law. The air heat capacity was taken from the COMSOL Multiphysics® materials library, whereas the argon heat capacity was taken as a constant (520 J/kg/K). The thermal conductivity of both gases, as well as the viscosity of argon, which is needed for the Nu number computation, are modelled according to Sutherland's law[12]. The properties of the insulation material (see Figure 2) are experimentally unknown and, therefore, are arbitrarily selected: zero electrical conductivity, density 10^3 kg/m^3, heat capacity 10^3 J/kg/K, emissivity 0.85, and thermal conductivity 10 W/m/K. Structural steel properties from the material library were used for the steel shell. Its hemispherical emissivity was taken as for the iron oxide Fe_2O_3[13]. The properties of refractory materials are taken from material data sheets provided by the refractory supplier[14]: Elite Cast 1400 INS for the external layer of the refractory, Elite ATB Cast 1750 for the internal body refractory, and Elite BA Cast 1800 INS for the internal roof refractory (see Figure 1). The calcium silicate board properties were obtained from the technical data sheet for the MB1000 Special material[14]. The thermal conductivity (in W/m/K) was interpolated as a function of T (in K):

$$k_{MB1000} = 9.7344\times10^{-9}\cdot T^2 + 2.5007\times10^{-6}\cdot T + 2.0106\times10^{-2}$$

Finally, the properties of the ceramic fiber blanket were modelled according to the specifications of Fibermax® Matte for a density of 130 kg/m^3. The heat capacity was estimated based on the composition.

6. Numerical results and discussion

6.1. Reduction vessel preheating and optimization of the heating rod geometry

Numerical simulations show that input power above 0.4 MW will be sufficient to preheat the empty reduction vessel up to 1600°C in less than 4 h (see Figure 7). However, even at 0.4 MW input power, dangerous temperatures above 2500°C were reached (see Figure 8). Increasing the heating rod emissivity decreases its maximum temperature $T_{hr,max}$ (see Figure 9) but is not sufficient to be below 2500°C. The natural gas convection in the crucible or the heat

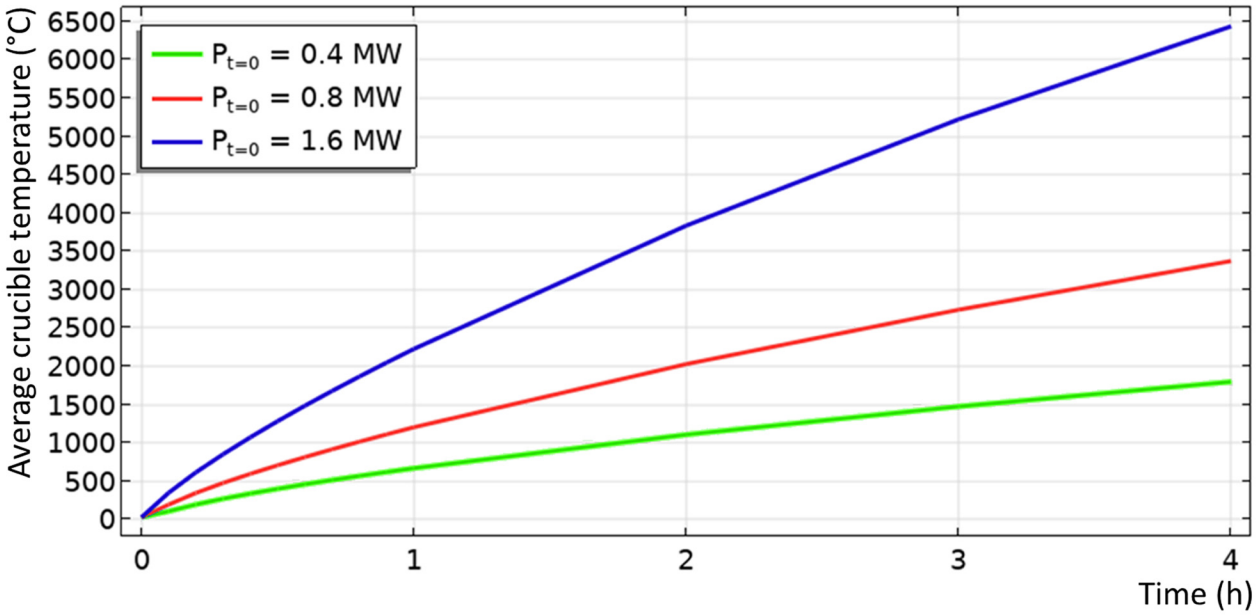

Figure 7. Computed average crucible temperature as function of time for different input power.

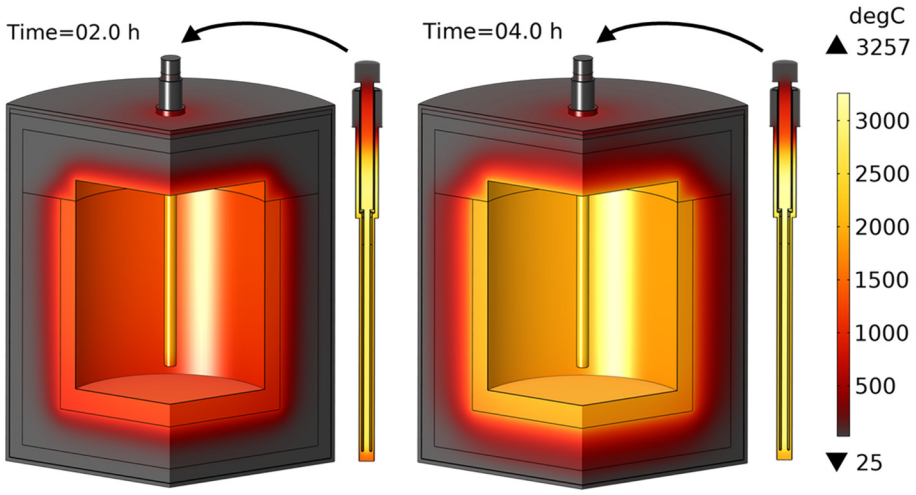

Figure 8. Temperature field for the input power of 0.4 MW and graphite emissivity of 0.5.

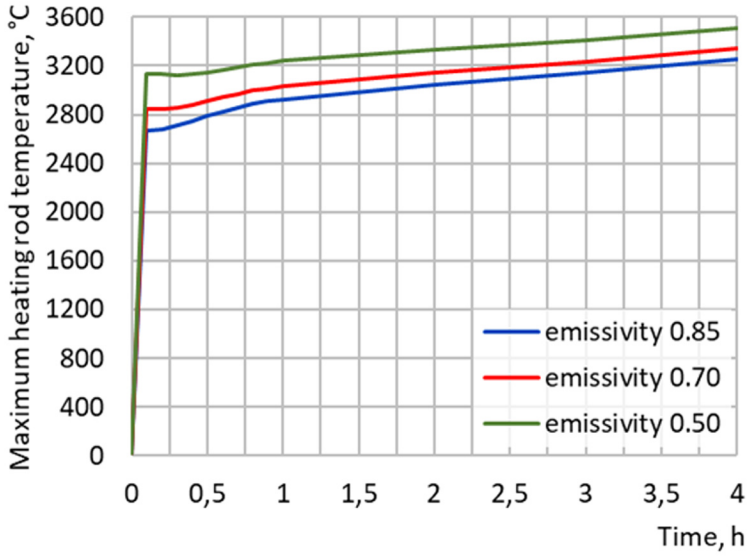

Figure 9. Maximum heating rod temperature at 0.4 MW input power for different graphite emissivity.

loss due to a protective gas flow through the crucible have an almost negligible influence on $T_{hr,max}$. Thus, the heating rod geometry was optimized by varying the three parameters a, b, c (see Figure 2) to satisfy 3 criteria:

1) The historical maximum power dissipation of the three heating rods should not exceed the maximum transformer power.

2) The average crucible temperature should reach 1600°C in less than 4 hours.

3) The maximum heating rod temperature $T_{hr,max}$ should not exceed 2500°C.

The result of such optimization shows that the delta (D) connection of heating rods (see Figure 4) should be avoided

as it delivers too much power and overheats the rods, even for the minimum available transformer voltage. Instead, a star (Y) connection of the heating rods should be used. In this case, when a minimum line voltage U_L of 105 V (as per available electrical equipment) is provided, the optimum geometry parameters are found to be

$$a = 50\,\text{mm}, \quad b = 2\,\text{mm}, \quad c = 15\,\text{mm}$$

With this heating rod geometry, the temperature field after 4 h of vessel preheating is shown in Figure 10: maximum heating rod temperature is below 2408°C, whereas average crucible temperature is above 1600°C. The transformer delivers between 337 and 410 kW of heating power, depending on the heating rod temperature at each moment in time. Note that in practice, in addition to the above three satisfied optimization criteria, there is also a mechanical strength requirement: the minimum thickness of the graphite parts must be greater than 1 cm. It can be seen that thickness b does not satisfy this criterion and becomes even thinner as the line voltage increases. Nevertheless, the optimized geometry of the rods will be used in further computations to study other thermal and electrical aspects of the reduction vessel design.

6.2. Charge heating with available transformer

Below, we present the results of the charge heating modeling with submerged heating rods powered by the available transformer: U_L = 105 V. The previously computed preheated state served as the initial condition, initial slag temperature was 1650°C, initial metal temperature was 800°C. Two cases were investigated: **Case 1:** only the slag was charged, **Case 2:** both the slag and metal were charged. In **Case 1** there was no chemical reaction, and the vessel was heated only by an electrical heat source. Figure 11 shows the computed temperature fields before and after 30 min of heating. As one can see, the temperature inside heating rods rises to 5103°C because of high electric currents passing through them (see Figure 12). The current goes down the internal graphite cylinder of the heating rod, and then, instead of going up through the external graphite cylinder, it prefers to pass through the slag volume and graphite crucible towards the two other graphite rods, which are also submerged into the slag. Apparently, this path is less resistive and creates a short circuit between heating rods. The effective line current I_L approaches 10^4 A, which is two times higher than the allowed transformer's maximum, and therefore, is dangerous for electrical equipment. In addition, as the slag temperature increases owing to heating, its electrical conductivity increases, which results in further growth of the electric current over time. To conclude **Case 1**, the presence of slag in the vessel resulted in a short circuit between heating rods, in dangerous transformer currents, and in graphite overheating above 2500°C. A similar conclusion was made for **Case 2** when both slag and metal were charged. The heat produced by the reaction and the high conductivity of the metal did not improve this situation.

6.3. Charge heating with reduced line voltage

Let us consider the worst-case configuration in which both the slag and metal are charged into the vessel. In this case, we can try to reduce the effective line voltage U_L to provide a reasonable electric power input and avoid the above-mentioned problems of excessive current and graphite overheating. The duration of the aluminothermic reduction was assumed to be 20 min, during which the reaction energy was released

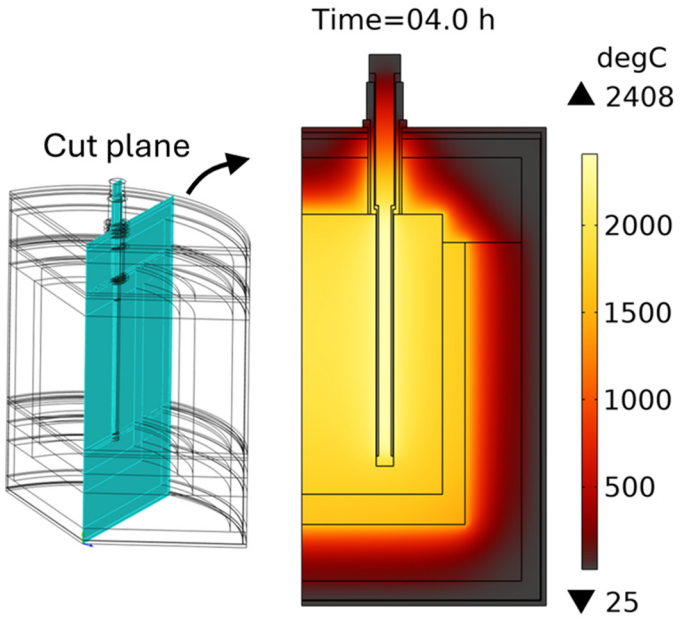

Figure 10. Temperature field after 4 hours of reduction vessel preheating with an optimized geometry of heating rods. Line voltage is 105 V.

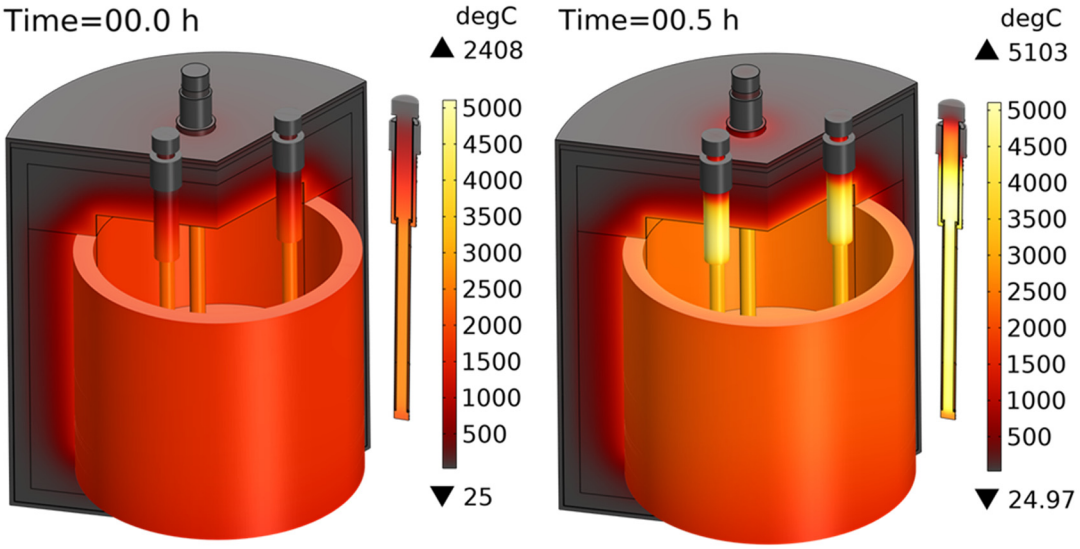

Figure 11. Temperature field when only slag is charged into the reduction vessel. Line voltage is 105 V.

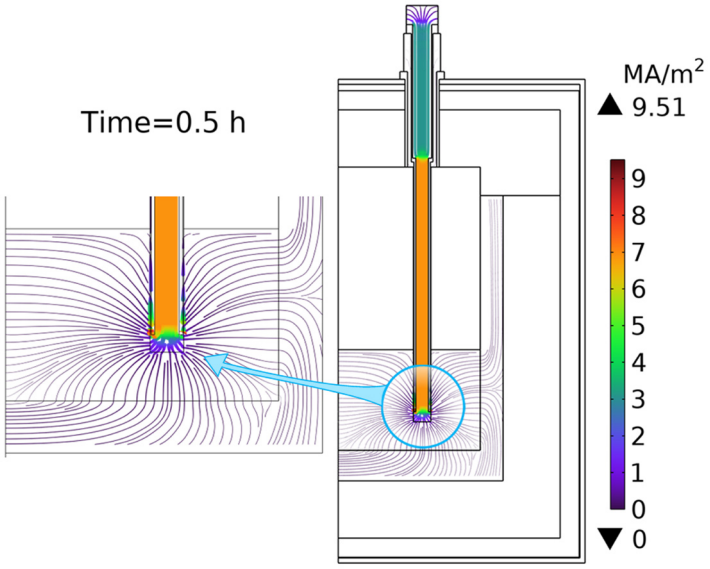

Figure 12. Map of the electric current density when only slag is charged into the vessel. Line voltage is 105 V.

at the slag-metal interface. By studying the influence of the line voltage U_L on the modelling results, it was found that a line voltage below 40 V is acceptable for vessel charge heating with three heating rods submerged in the melt. Figure 13 shows the resulting evolution of the vessel temperature field. The results show that the heating rod temperature decreases with time as the electrical input power is below that provided during the preheating stage. The crucible temperature slowly increased with time owing to the joint contribution of the electrical and chemical (≈ 890 kW) power input. If such a transformer setting with U_L = 40 V is possible, it would result in approximately 180 kW of electrical power input, which would be enough to compensate for heat losses and to maintain the charge above its melting point over a long period of time to maximize the chemical reaction output. In this hypothetical vessel configuration, the heating rod temperature remained below the maximum acceptable graphite temperature of 2500°C, and the effective line current I_L did not exceed the allowed maximum provided by the transformer.

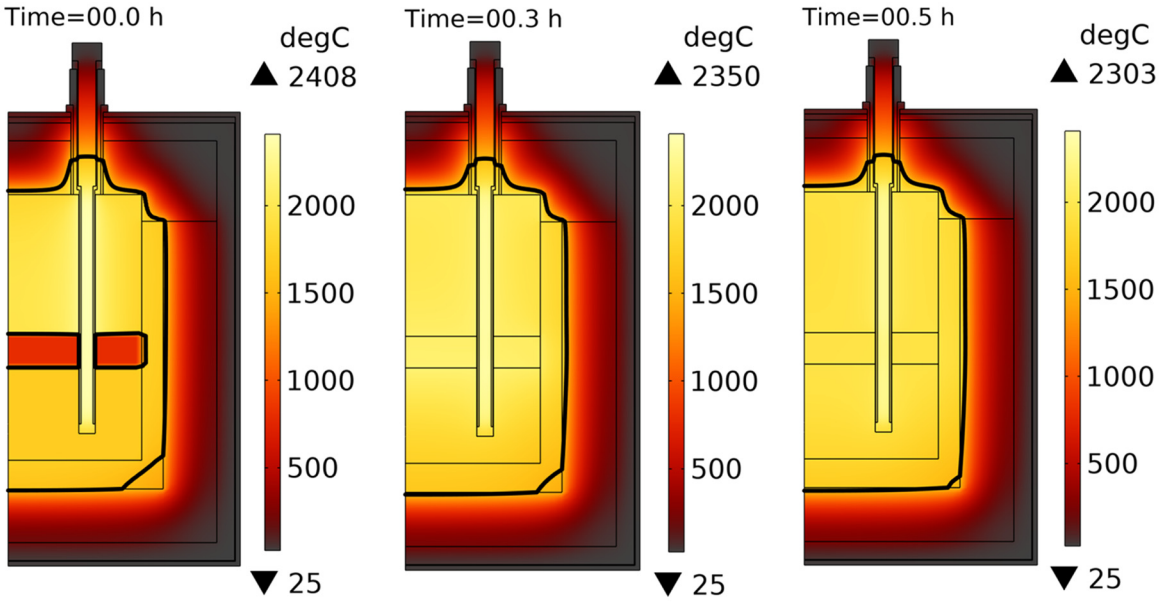

Figure 13. Temperature field evolution when both slag and metal are charged into the reduction vessel. Line voltage is 40 V. Thick black line represents the slag melting temperature isoline (1540°C).

6.4. Aluminothermic reduction with no external heating

The results of modelling the situation when no electrical power was provided are shown in Figure 14. In this case, the maximum temperature in the vessel reduced faster with time than in the case with nonzero electrical power. Nevertheless, the aluminothermic reduction power alone is sufficient to maintain the melt in a liquid state for at least 30 min.

6.5. Reduction vessel preheating and charge heating with a single heating rod

In the above results, we have seen that heating the vessel charge with three submerged heating rods is problematic because the electrically conducting slag and metal create a short circuit between the rods, which results in thermal and electrical damage to the reduction vessel and transformer. Therefore, in this section, a configuration with a single heating rod submerged in the melt at the center of the vessel is studied, as it excludes the possibility of a short circuit between the three electrical phases. The electrical circuit was modified as shown in Figure 15. The analysis shows that avoiding the transformer damage, the power dissipated in a single heating rod should not exceed 50% of the nominal transformer power for a given line voltage U_L. Numerical testing of the feasibility of vessel preheating with a single heating rod gives an optimum line voltage of U_L = 70 V, which is below the possible minimum of 105 V as per the available electrical equipment. According to the model, a line voltage of 70 V would result in an optimum time for vessel preheating up to 1600°C with heating rod temperature not exceeding 2500°C (see Figure 16 and Figure 17). However, it still requires 12 h of preheating instead of the desired 4 h, because the power provided by the transformer in this case is approximately 186 kW. Thus, preheating the reduction vessel with one heating rod can be considered impractical and unrealizable with the currently available equipment at MINTEK.

Modelling of charge heating with a single heating rod submerged into the melt shows that further reduction of line voltage is needed to avoid thermal damage to the heating rod. In the case of only charged slag, a line voltage U_L below 65 V is required, whereas in the case of both charged slag and metal, a line voltage U_L below 48 V would be safe. The need for voltage reduction can be explained by the increase in the line current I_L when the heating rod is submerged in the molten charge. This occurs because the electrical resistance between the heating rod terminals is reduced owing to the nonzero electrical conductivity of the slag and metal layers. The numerical model demonstrates how the electric current bypasses the submerged portion of the heating rod via the electrically conducting charge volume, as shown in Figure 18. Thus, a short circuit is created between the lower and upper submerged parts of the external graphite cylinder of the heating rod, which increases the power input and eventually overheats the heating rod.

7. Conclusions

The present numerical model predicts that available electrical equipment is sufficient for preheating the empty reduction vessel up to 1600°C in less than 4 h. Owing to the model, the geometry of the heating rod was optimized to maintain its temperature below 2500°C. However, it was found that the electrical function of the reduction vessel is strongly affected by

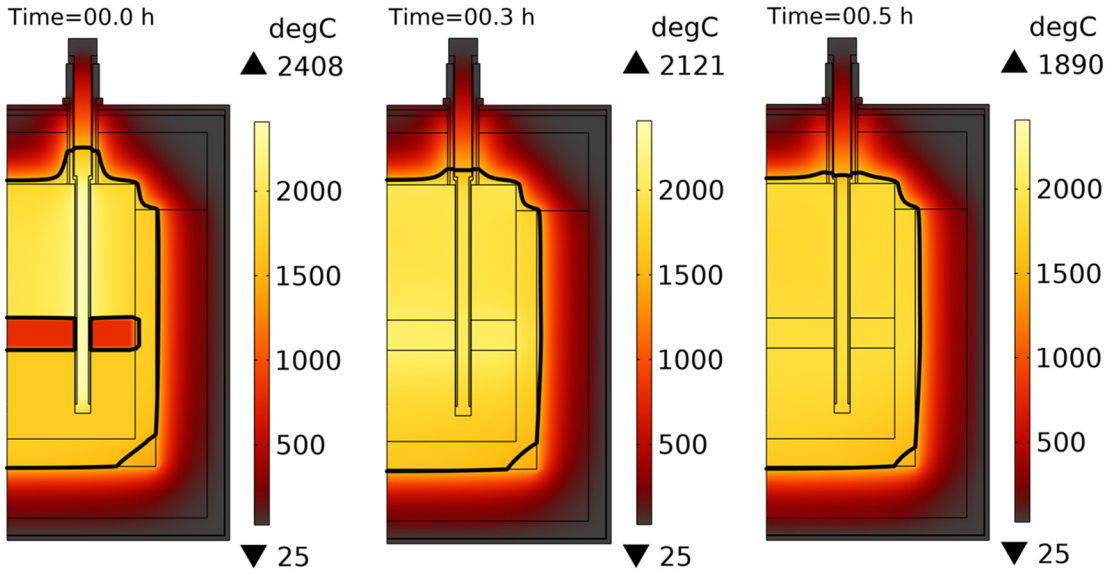

Figure 14. **Temperature field evolution when both slag and metal are charged into the reduction vessel with no electrical power input. Thick black line represents the slag melting temperature isoline (1540°C).**

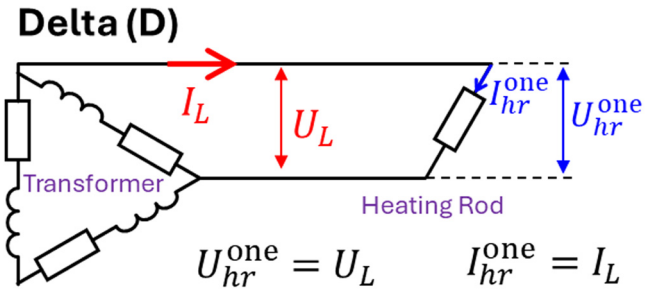

Figure 15. **One heating rod connection.**

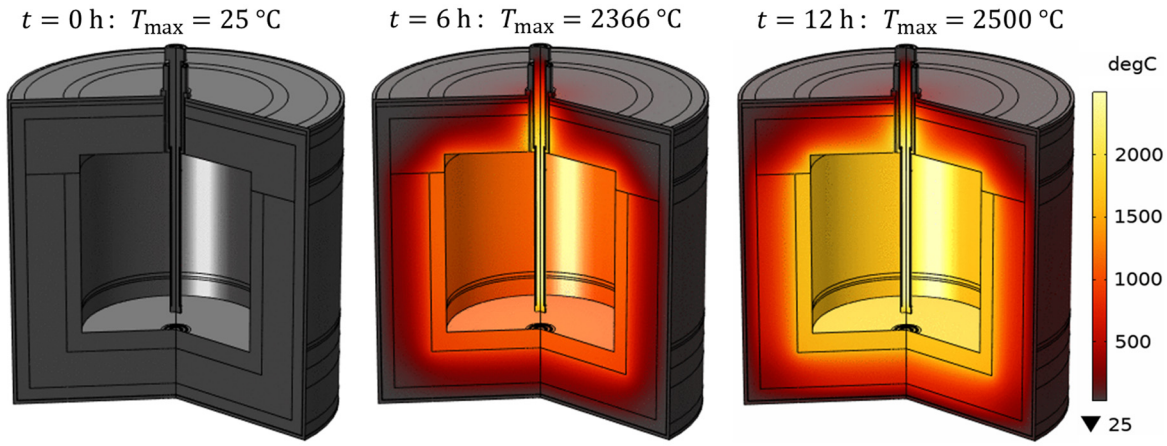

Figure 16. **Time evolution of the temperature field during vessel preheating with a single heating rod at U_L = 70 V.**

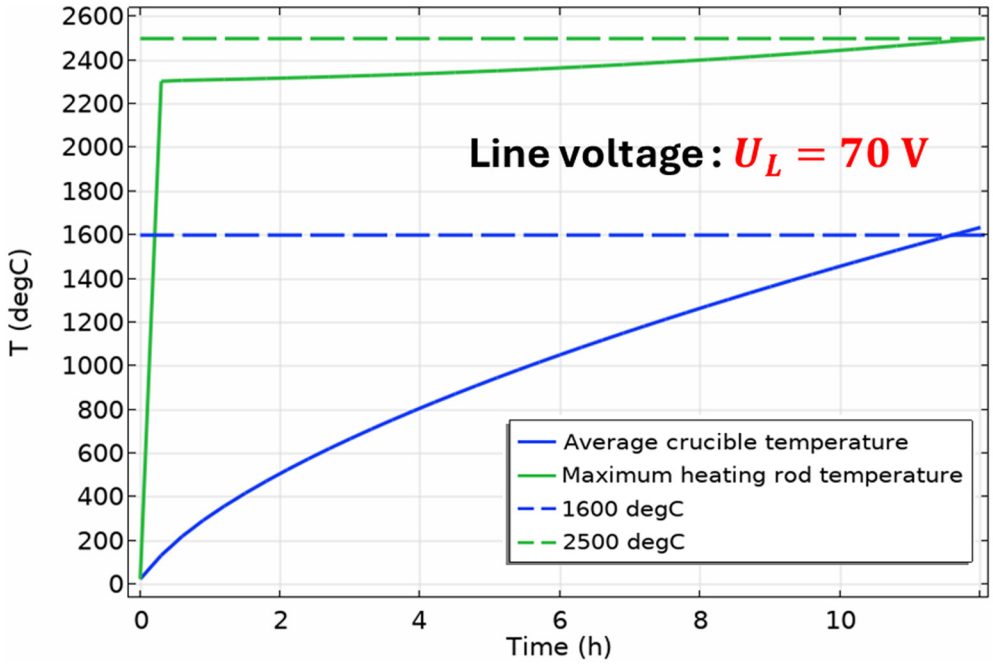

Figure 17. **Time evolution of the average crucible temperature and of the maximum heating rod temperature in a single-heating-rod configuration of the vessel.**

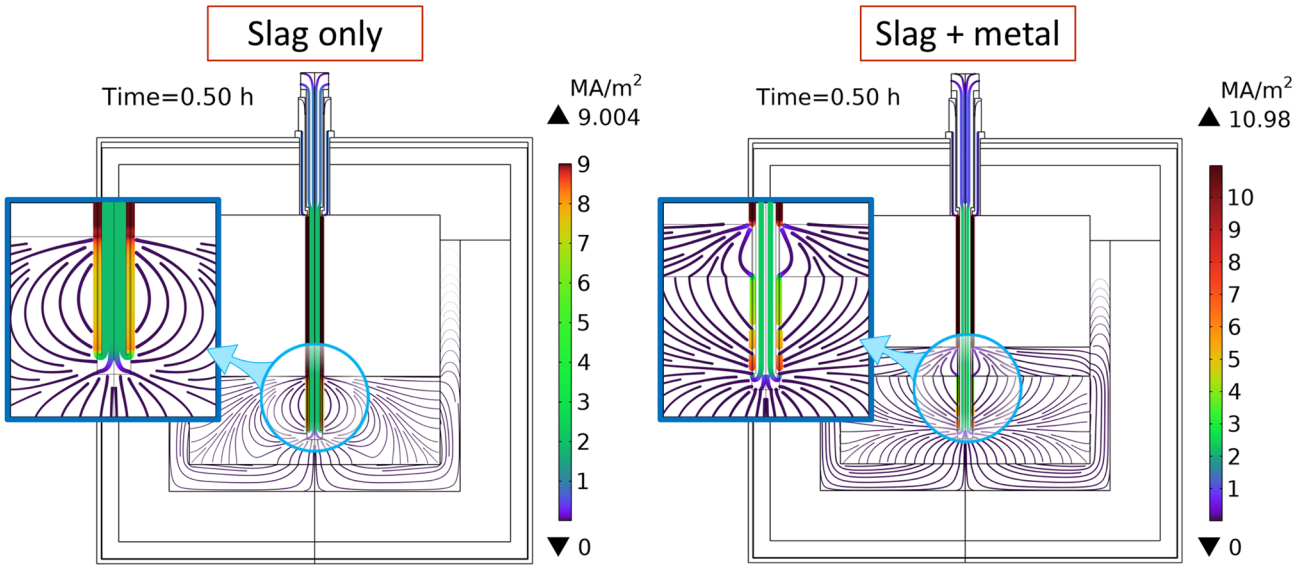

Figure 18. **Map of electric current density when heating rod is submerged into the vessel charge at U_L = 70 V.**

the presence of the vessel charge, as both slag and metal are electrically conducting materials. The configuration where three heating rods are submerged into the molten charge is not acceptable, as it leads to a short circuit between heating rods, to an effective line current I_L exceeding the allowed maximum provided by the transformer, and to the graphite overheating above the maximum acceptable temperature of 2500°C. The reduction of the line voltage down to 40 V was found to be sufficient to avoid electrical and thermal damage to the reduction vessel in the configuration with three heating rods

submerged into the melt. Similarly, in the single-heating-rod configuration, vessel preheating is possible when the line voltage U_L does not exceed 70 V, slag heating is possible when U_L < 65 V, and slag and metal heating is possible when U_L < 48 V. Otherwise, thermal damage to the graphite heating rod is unavoidable. Because reducing the line voltage below 105 V might not be possible, as it requires the replacement of the existing transformer, a numerical study with no electrical power input has been performed. This shows that the aluminothermic reduction power alone is sufficient to maintain the melt in a liquid state for at least 30 min. If electrical insulation of heating rods from the melt could be found, it would result in normal functioning of the electrical circuit, even with the original transformer settings. However, in this case, overheating of the graphite rods might be possible during the aluminothermic reduction process due to the reaction heat. Thus, according to the model, switching off the electrical power supply is recommended for the duration of the aluminothermic reduction process when the heating rods are submerged in the melt.

Ethics and consent

Ethical approval and Consent were not required.

Data and software availability

Repository: Zenodo. Dataset title: "Refractory materials used in the numerical model of an aluminothermic reduction vessel"

https://doi.org/10.5281/zenodo.13880179[14].

This project contains the following underlying data:

Data file 1: "Elite ATB Cast 1750.png" (Data sheet for the properties of Elite ATB Cast 1750 material)

Data file 2: "Elite BA Cast 1800 INS.png" (Data sheet for the properties of Elite BA Cast 1800 INS material)

Data file 3: "Elite Cast 1400 INS.png" (Data sheet for the properties of Elite Cast 1400 INS material)

Data file 4: "MB1000 Special.png" (Data sheet for the properties of MB1000 Special material)

Data are available under the terms of the Creative Commons Attribution 4.0 International licence.

No extended data associated with this article.

References

1. McEligot D, Swank WD, Cottle DL, *et al.*: **Thermal properties of G-348 graphite**. Idaho National Lab.(INL), Idaho Falls, ID (United States), 2016.
Publisher Full Text
2. Smith DS, Alzina A, Bourret J, *et al.*: **Thermal conductivity of porous materials.** *J Mater Res.* 2013; **28**(17): 2260–2272.
Publisher Full Text
3. Entegris Inc: **Properties and Characteristics of graphite, for the semiconductor industry**. 2013.
4. Leitner M, Leitner T, Schmon A, *et al.*: **Thermophysical properties of liquid aluminum.** *Metall Mater Trans A.* 2017; **48**(6): 3036–3045.
Publisher Full Text
5. Assael MJ, Armyra IJ, Brillo J, *et al.*: **Reference data for the density and viscosity of liquid cadmium, cobalt, gallium, indium, mercury, silicon, thallium, and zinc.** *J Phys Chem Ref Data.* 2012; **41**(3): 033101.
Publisher Full Text
6. Bohdansky J, Schins HEJ: **Surface tension and density of the liquid earth alkaline metals Mg, Ca, Sr, Ba.** *J Inorg Nucl Chem.* 1968; **30**(9): 2331–2337.
Publisher Full Text
7. Xin J, Gan L, Jiao L, *et al.*: **Accurate density calculation for molten slags in SiO_2-Al_2O_3-CaO-MgO systems.** *ISIJ Int.* 2017; **57**(8): 1340–1349.
Publisher Full Text
8. Tang K, Gouttebroze S, Ma X, *et al.*: **Representation of the multiphysical properties of SiO2-Al2O3-CaO slags by deep neural networks.** In: *Proceedings of the 16th International Ferro-Alloys Congress (INFACON XVI).* (virtual). 2021.
Publisher Full Text
9. Tang K, van der Eijk C, Gouttebroze S, *et al.*: **Rheological properties of Al_2O_3--CaO--SiO_2 slags.** *Calphad.* 2022; **77**: 102421.
Publisher Full Text
10. Dinsdale AT, Quested PN: **The viscosity of aluminium and its alloys--a review of data and models.** *J Mater Sci.* 2004; **39**: 7221–7228.
Publisher Full Text
11. Mills KC, Yuan L, Jones RT: **Estimating the physical properties of slags.** *J S Afr Inst Min Metall.* 2011; **111**(10): 649–658.
Reference Source
12. COMSOL Documentation: **Sutherland's law**.
Reference Source
13. Burgess GK, Foote PD: **The emissivity of metals and oxides. IV. Iron oxide.** *J Wash Acad Sci.* 1915; **5**(11): 377–378.
Reference Source
14. Semenov S: **Refractory materials used in the numerical model of an aluminothermic reduction vessel**. 2 October, 2024.
http://www.doi.org/10.5281/zenodo.13880179

Open Peer Review

Current Peer Review Status: ✔ ✔

Version 1

Reviewer Report 29 December 2025

https://doi.org/10.21956/openreseurope.20105.r62728

© **2025 Antoni M.** This is an open access peer review report distributed under the terms of the Creative Commons Attribution License, which permits unrestricted use, distribution, and reproduction in any medium, provided the original work is properly cited.

✔ **Mickaël Antoni**
Aix-Marseille Université, Marseille, France

This article presents numerical investigations of vessel designs intended for high-temperature chemical reactors, involving both electrical and thermal transfer processes. It aims to help the understanding of experimental conditions needed for running conducted with a pilot scale facility for the production of metallurgical-grade silica via aluminothermic reduction, a method that offers an improved carbon footprint (particularly in terms of CO_2 emissions) compared to traditional carbothermic techniques.

The main objective is to optimize high-temperature processes using models and simulations performed with COMSOL Multiphysics, accounting material safety constraints, electrical supply characteristics and energy balance. Three specific goals are pursued:
· To verify whether a 4-hour preheating phase can bring the bath of preheat the empty vessel up to 1,600 °C.
· To assess the feasibility of regulating the heating of the molten bath using three graphite electrodes.
· To analyze the risks associated with the formation of solid slag during the aluminothermic reduction phase (slag solidification).
The article is clear and well-written. The illustrations are consistent with the provided explanations. The system geometry, including the structure and dimensions of the crucible and graphite electrodes, is described in detail. The numerical method is presented concisely yet sufficiently: the COMSOL modules used to describe the physical properties of the materials phenomena are mentioned, as are the discretization scheme (linear Lagrangian finite elements) and the numerical time integration scheme (BDF).

The core section of the article focuses on modeling the entire experimental facility, including the crucible structure, graphite electrodes, and molten bath. The description of the equations used to model electrical and radiative phenomena is appropriate and detailed. Particular attention is given to the physicochemical properties of the materials, especially those of graphite and the emissivity value of the heating rods.

Simulations were conducted for four distinct scenarios, including reduced voltages and the use of a single graphite rod. The results demonstrate that the available equipment can indeed achieve 1,600 °C in less than 4 hours while avoiding exceeding 2,500 °C at the vessel level. However, the three-electrode setup in the presence of a molten bath poses a risk of short circuits, potentially compromising both the power source and the vessel structure. In contrast, the single-rod configuration allows risk limitation within specific voltage ranges.

The authors mention the limitations of the models, particularly the use of empirical descriptions for convective phenomena and the calculation of the heat transfer coefficient. A turbulent CFD model would substantially improve our understanding of convective heat transfer and the transport of chemical species within the molten bath. The properties of the graphite rods insulation were chosen arbitrarily but as realistically as possible. Figure 13 indicates a potential risk of exceeding the working temperature of refractory materials around the rods insulation. Analyzing this aspect of the thermal vessel design in more detail would enable the prediction of suitable thermal properties and dimensions of the insulation material. Another simplifying assumptions was that the aluminothermic reaction rate remained constant for the full 20 minutes of the reaction, resulting in a constant exothermic heat power. In perspective, a more realistic decaying reaction rate could be implemented based on the depletion of reacting species, for example. These points provide interesting openings and perspectives for future research.

Despite these limitations, this article remains robust and offers a valuable contribution to the use of low-carbon processes, a major challenge in metallurgy. The results and perspectives presented make this article relevant to the scientific community.

Is the work clearly and accurately presented and does it cite the current literature?
Partly

Is the study design appropriate and does the work have academic merit?
Yes

Are sufficient details of methods and analysis provided to allow replication by others?
Yes

If applicable, is the statistical analysis and its interpretation appropriate?
Not applicable

Are all the source data underlying the results available to ensure full reproducibility?
Yes

Are the conclusions drawn adequately supported by the results?
Yes

Competing Interests: No competing interests were disclosed.

Reviewer Expertise: Simulation of heat and mass transfer mechanisms (CFD), dispersed systems (emulsions, aerosols), corium-concrete interaction, instrumentation.

I confirm that I have read this submission and believe that I have an appropriate level of expertise to confirm that it is of an acceptable scientific standard.

Reviewer Report 10 January 2025

https://doi.org/10.21956/openreseurope.20105.r48721

© **2025 Benzesik K.** This is an open access peer review report distributed under the terms of the Creative Commons Attribution License, which permits unrestricted use, distribution, and reproduction in any medium, provided the original work is properly cited.

Kagan Benzesik
Istanbul Technical University, Istanbul, Turkey

The article *"Numerical Model of Aluminothermic Reduction Vessel Preheating and Charge Heating with Graphite Heating Rods"* investigates the optimization of reduction vessels used for sustainable silicon production. Using COMSOL Multiphysics, the authors model the thermal and electrical performance of vessels during preheating and charge heating processes, focusing on graphite heating rods powered by a three-phase transformer. The study finds that preheating the vessel to 1600°C within 4 hours is feasible with current equipment, but submerged heating rods cause short circuits, transformer overloading, and graphite overheating. The model suggests that reducing line voltage to 40V or insulating the rods could mitigate these issues.
The research contributes to the SisAl Pilot EU project, promoting low-carbon aluminothermic reduction methods.
This article presents a well-structured and impactful study that combines rigorous numerical modeling with practical applications in sustainable metallurgical processes. The insights gained from optimizing reduction vessel designs and identifying challenges like heating rod overheating or transformer limitations offer valuable guidance for both researchers and industry professionals. By addressing the suggested improvements—such as enhancing readability, contextualizing findings within broader research, and proposing future directions—the article has the potential to make a significant contribution to the field. Overall, the work stands as a promising advancement in the pursuit of low-carbon metallurgical technologies and aligns effectively with global sustainability goals.

Is the work clearly and accurately presented and does it cite the current literature?
Partly

Is the study design appropriate and does the work have academic merit?
Yes

Are sufficient details of methods and analysis provided to allow replication by others?
Yes

If applicable, is the statistical analysis and its interpretation appropriate?
Not applicable

Are all the source data underlying the results available to ensure full reproducibility?
Yes

Are the conclusions drawn adequately supported by the results?
Yes

Competing Interests: No competing interests were disclosed.

Reviewer Expertise: metallothermic reduction, combustion synthesis, self propagating high temperature synthesis

I confirm that I have read this submission and believe that I have an appropriate level of expertise to confirm that it is of an acceptable scientific standard.